Inorganic Chemistry

Article

pubs.acs.org/IC

Assignment of Metal–Ligand Modes in Pt(II) Diimine Complexes Relevant to Solar Energy Conversion

Stewart F. Parker,*[,†] Keith Refson,[‡] Robert D. Bennett,[§] Jonathan Best,[§] Mikhail Ya. Mel'nikov,[∥] and Julia A. Weinstein*[,§]

[†]ISIS Facility and [‡]Computational Materials Science Group, STFC Rutherford Appleton Laboratory, STFC, Didcot, Chilton, Oxfordshire, OX11 0QX, U.K.

[§]Department of Chemistry, University of Sheffield, Sheffield S3 7HF, U.K.

[∥]Department of Chemistry, Moscow State University, Moscow, Russia

Supporting Information

ABSTRACT: This work describes a comprehensive assignment of the vibrational spectra of the platinum(II) diimine bisthiolate and chloride complexes as a prototype structure for a diversity of Pt(II) diimine chromophores. The dynamics and energy dissipation pathways in excited states of light harvesting molecules relies largely on the coupling between the high frequency and the low frequency modes. As such, the assignment of the vibrational spectrum of the chromophore is of utmost importance, especially in the low-frequency region, below 500 cm^{-1}, where the key metal–ligand framework modes occur. This region is experimentally difficult to access with infrared spectroscopy and hence frequently remains elusive. However, this region is easily accessible with Raman and inelastic neutron scattering (INS) spectroscopies. Accordingly, a combination of inelastic neutron scattering and Raman spectroscopy with the aid of computational results from periodic-DFT and the mode visualizations, as well as isotopic substitution, allowed for an identification of the modes that contain significant contributions from Pt–Cl, Pt–S, and Pt–N stretch modes. The results also demonstrate that it is not possible to assign transition energies to "pure", localized modes in the low frequency region, as a consequence of the anticipated severe coupling that occurs among the skeletal modes. The use of INS has proved invaluable in identifying and assigning the modes in the lowest frequency region, and overall the results will be of assistance in analyzing the structure of the electronic excited state in the families of chromophores containing a Pt(diimine) core.

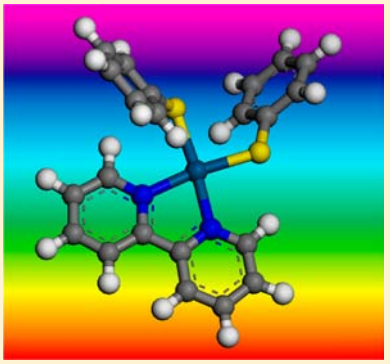

I. INTRODUCTION

In solar energy conversion, the key transient is a charge-separated excited state which is formed as a result of photoinduced charge transfer following the initial absorption of light.[1] Transition metal complexes are often used in artificial systems for solar energy conversion because of their intense absorption in the visible region and the charge transfer nature of the lowest excited state.[2] Among those systems, Pt(II) diimine complexes with ancillary anionic ligands are frequently used as a core chromophoric part of extensive molecular assemblies designed for photoinduced electron transfer, dye-sensitized solar cells, and hydrogen production.[3] Accordingly, the properties of their excited state have been studied in detail.[4] However, the structure of the charge transfer excited state in those systems, and its difference from the ground state structure, is yet to be resolved. Another important, and as yet unanswered question, in relation to charge-transfer excited states is elucidation of their deactivation pathways. It is widely accepted that low frequency vibrational modes play an important role in the vibrational energy redistribution and energy dissipation in the excited state.[5] In this context, metal–ligand framework vibrational modes, such as Pt–S, Pt–N or Pt–Cl vibrations, are of major importance in fundamental questions of structure and dynamics. Vibrational spectroscopy, time-resolved infrared and time-resolved resonance Raman spectroscopy, is one of the few direct tools which can assist in answering those questions as it provides bond-specific structural information.[6]

The assignment of the ground state vibrational spectrum is an essential first step toward the assignment of the excited state spectra. This work describes a study aimed at a comprehensive assignment of the vibrational spectra of the ground state of the platinum 2,2′-bipyridine (bpy) thiolate (SPh) complex, Pt(bpy)$(SPh)_2$ (see Scheme 1 for the structure) as a prototype structure for a diversity of Pt(II) diimine chromophores. Its precursor Pt(bpy)Cl_2 was studied to assist with identifying the modes associated with the S–Ph group. The modes of particular interest, Pt–S, Pt–N, and Pt–Cl vibrations,[7] all lie below ∼500 cm^{-1}. This region is experimentally difficult to access with infrared spectroscopy and hence remained elusive until now. However, this region is readily accessible with

Received: May 28, 2012
Published: August 31, 2012

Scheme 1. Compounds Investigated in This Study: Pt(*NN*)R_2, where NN = d_8-2,2′-bipyridine, or h_8-2,2′-bipyridine, and R = Cl or −S-Ph

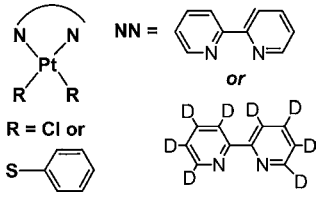

Raman spectroscopy and inelastic neutron scattering (INS) spectroscopy; hence, these techniques were employed in this study.

Inelastic neutron scattering (INS) is a powerful technique that is complementary to infrared and Raman spectroscopies.[8] For the present work, the key feature is that there are no selection rules and all modes are allowed. The intensities in the INS spectrum are proportional to the incoherent cross section and the amplitude of motion of the atoms involved in the mode. For ^{1}H normal hydrogen, the cross section of 80.27 barns (1 barn =1 × 10^{-28} m^2) is ∼20-fold larger than for any other atom or isotope (cf. ^{2}H 2.05 barns) and since ^{1}H is the lightest isotope of the lightest element, the amplitude of motion is largest for this isotope, thus the technique emphasizes the vibrational modes involving hydrogen motions. INS can provide information on the low-energy region of the vibrational spectrum—as low as 16 cm^{-1}—which is not accessible with standard Raman methods. There is a natural synergy with computational methods in that to generate the INS spectrum, all that is required are the displacements of each atom in each mode.[8] INS has been used extensively to investigate transition metal hydrides;[9] however, the application to inorganic complexes in general is much more limited,[10] although a recent study reported a detailed vibrational study of cis-platin, [*cis*-$PtCl_2(NH_3)_2$].[11]

Mode assignment was done with the aid of isotopic substitution using fully deuterated d_8-2,2′-bipyridine as a ligand, that is, Pt(d_8-bpy)$(SPh)_2$, and periodic density functional theory (periodic-DFT) calculations.

II. EXPERIMENTAL SECTION

A. Compounds. Pt(bpy)$(SPh)_2$ and the yellow form of Pt(bpy)Cl_2 were prepared as described previously.[12] Pt(d_8-bpy)$(SPh)_2$ was prepared from d_8-2,2′-bipyridine, kindly provided by Prof. H. Vos, Dublin City University, Ireland, and Prof. O. Poizat, Université de Lille I, France. Bipyridine (Aldrich, 99%) was used as received; diphenyl disulfide (Ph−S−S−Ph, Aldrich, 99%) was recrystallized from ethanol.

B. Vibrational Spectroscopy. The INS spectra were recorded using the high resolution (∼1.25% E/E) broadband (16−4000 cm^{-1}) spectrometer TOSCA[13] at the pulsed spallation neutron source ISIS[14] (Chilton, U.K.). TOSCA is an inverted geometry time-of-flight spectrometer where a pulsed, polychromatic beam of neutrons illuminates the sample at 17 m from the source. The scattered neutrons are Bragg reflected by a pyrolytic graphite analyzer, and those with a final energy of ∼32 cm^{-1} are passed to the ^{3}He detector bank. Energy transfer and spectral intensity is then calculated using standard programs to convert to the conventional $S(Q)$. The samples, ∼2 g, were held in aluminum sachets, cooled to ∼20 K, and the spectra were recorded for 6−12 h. The INS spectra are available from the INS database at http://wwwisis2.isis.rl.ac.uk/INSdatabase/. Raman spectra were recorded with a Renishaw inVia Raman spectrometer which is fiber-optically coupled to a Raman microscope. The excitation wavelength was 785 nm. Spectra were recorded from 100−3200 cm^{-1}, the lower limit is set by the notch filter used to reject the Rayleigh scatter and the high limit by the falloff in the CCD response. Typical conditions were 5−10 min measurement time with ∼10 mW laser power at the sample and ∼4 cm^{-1} resolution. The instrument is described in detail elsewhere.[15]

C. Ab Initio Calculations. Periodic-DFT calculations were carried out using the plane wave pseudopotential method implemented in the CASTEP[16,17] code. Exchange and correlation were approximated using the PBE functional.[18] The plane-wave cutoff energy was 850 eV for PhSSPh and bpy, 720 eV for Pt(bpy)Cl_2 and 850 eV for Pt(bpy)$(SPh)_2$. Brillouin-zone sampling of electronic states was performed on 3 × 3 × 4 Monkhorst−Pack grid for PhSSPh and bpy, a 1 × 2 × 3 grid for Pt(bpy)Cl_2 and a 2 × 2 × 2 grid for Pt(bpy)$(SPh)_2$. The equilibrium structure, an essential prerequisite for lattice dynamics calculations was obtained by BFGS geometry optimization after which the residual forces were converged to zero within 0.0012 eV/A. Phonon frequencies were obtained by diagonalization of dynamical matrices computed using density-functional perturbation theory[17] (DFPT) and also to compute the dielectric response and the Born effective charges, and from these the mode oscillator strength tensor and infrared absorptivity were calculated. The Raman activity tensors were calculated using a hybrid finite displacement/DFPT method.[19] Transition energies for isotopic species were calculated from the dynamical matrix that is stored in the CASTEP checkpoint file using the PHONONS utility.[20] Calculation of the Raman spectrum of Pt(d_8-bpy)$(SPh)_2$ would have required a new DFPT calculation and so was not carried out. Some preliminary calculations were also carried out with Gaussian03.[21] For both CASTEP and Gaussian03, the atomic displacements enable visualization of the modes that aid assignments; they are also all that is required[8] to generate the INS spectrum using the program ACLIMAX.[22] We emphasize that all the spectra shown have *not* been scaled.

III. RESULTS

The focus of this paper is on the low energy region of the vibrational spectrum where the modes of interest, Pt−S, Pt−N, and Pt−Cl, occur. In this section we present the experimental INS and Raman spectra and the corresponding spectra generated from the CASTEP calculations for the region 0−800 cm^{-1}. The procedure adopted is to build up in complexity starting with the ligands, through Pt(bpy)Cl_2 and finally to Pt(bpy)$(SPh)_2$ and its d_8-bpy isotopomer. For each molecule, a comparison of the experimental and calculated structures is given in the Supporting Information together with a table of vibrational assignments.

A. Diphenyl Disulfide, PhSSPh. X-ray crystallography[23,24] shows that PhSSPh has a C_1 structure, (see inset to Figure 1). The calculated structure is in reasonable agreement with the crystallographic result, see Supporting Information, Table S1, although the S−S distance (2.009 Å calc., 2.028, 2.0343 Å obs.[23,24]) is slightly too short. All other bond distances are within 0.015 Å deviation of the experimental distances, and all the bond angles except one are within 1°, the exception is a S−S−C angle which differs by 1.8/1.6°. In particular, the dihedral angle between the phenyl rings is very well reproduced (85.0° calc., 84.2, 84.4° obs.[23,24]). We have also calculated the structure for an isolated PhSSPh molecule, where we have retained the same size unit cell but removed all the molecules except one. The reason for doing this reduction is that the cost of calculating the Raman intensities is very dependent on the number of atoms present, this procedure drastically reduces the computational time and hence cost. The structural parameters are very similar to those of the complete crystal, the only significant change is that the dihedral angle has increased to 91.2°. The calculation for the complete unit cell has one small imaginary mode (−31 cm^{-1}) that is an optic translation, which

dx.doi.org/10.1021/ic3011184 | *Inorg. Chem.* 2012, 51, 9748−9756

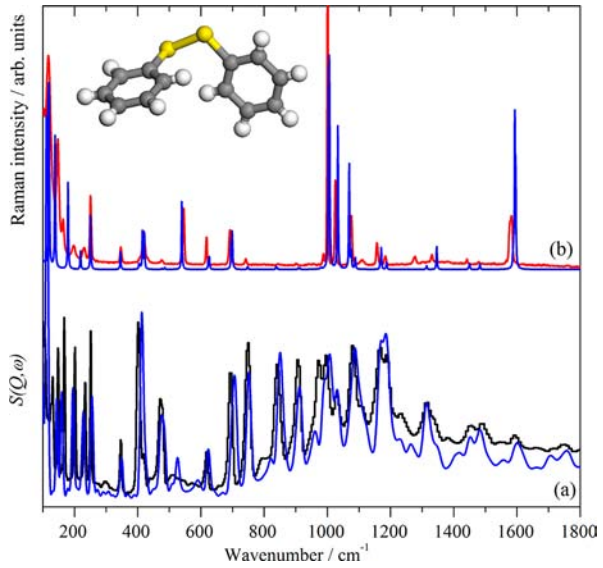

Figure 1. Observed and calculated (blue traces) (a) INS and (b) Raman spectra of diphenyl disulfide, PhSSPh.

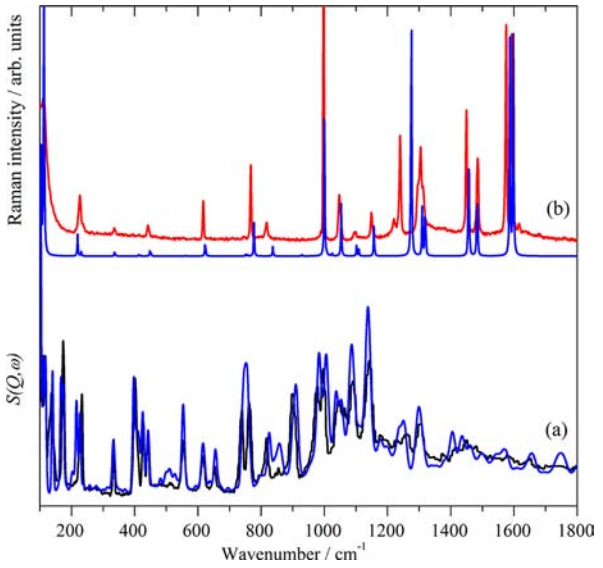

Figure 2. Observed and calculated (blue traces) (a) INS and (b) Raman spectra of transoid 2,2′-bipyridine, bpy.

is of no consequence for the present work. Figure 1 presents the observed and calculated INS and Raman spectra and show excellent agreement. Our assignments of the vibrational bands, Supporting Information, Table S2, are in agreement with previous work.[25−27]

B. 2,2′-Bipyridine, bpy. 2,2′-Bipyridine has a transoid, C_{2h}, structure in the gas phase[28] and in the solid state[29] whereas a cisoid, C_{2v}, structure is found in many metal complexes,[30] including those studied here. The structure is virtually unchanged between the gas phase and the solid state, and the calculated structure, with two molecules in the unit cell, is in good agreement with the literature data, see Supporting Information, Table S3. We have also calculated the spectra for the hypothetical cisoid structure in the same unit cell (but with only a single molecule in the unit cell, $Z = 1$) as for the experimental transoid structure. Bond distances and angles are almost unchanged by the rotation about the 2,2′ linkage. The observed INS and Raman spectra for the transoid structure of bpy are shown in Figure 2 and the INS spectrum of transoid 2,2′-bipyridine is compared to that calculated for the hypothetical cisoid structure in Figure 3. As may be expected, it can be seen that the match of observed and calculated spectra is much better for the transoid than the cisoid structure. Nonetheless, it does demonstrate the sensitivity of vibrational spectroscopy to the local structure. The vibrational spectra of bpy have been previously assigned for both the isolated molecule[31,32] and the crystal,[33,34] and our assignments, Supporting Information, Table S4, are largely in agreement with these previous assignments. The only significant exception is a mode that is clearly seen at 553 cm^{-1} in the INS spectrum that has not observed in either the infrared[33] or the Raman (see Figure 3b) spectra. The calculations correctly predict modes at 561 (A_g) and 564 cm^{-1} (B_g), which are formally Raman active and are out-of-plane ring deformations; however, they are calculated to have almost zero Raman intensity and were previously assigned at 442 (A_g) and 438 cm^{-1} (B_g). These latter two modes are now assigned as the inter-ring in-plane bend (previously at 410 (A_g) and 415 cm^{-1} (B_g)). CASTEP also correctly predicts the mode symmetry. For the cisoid, inspection of the modes shows that the external modes couple

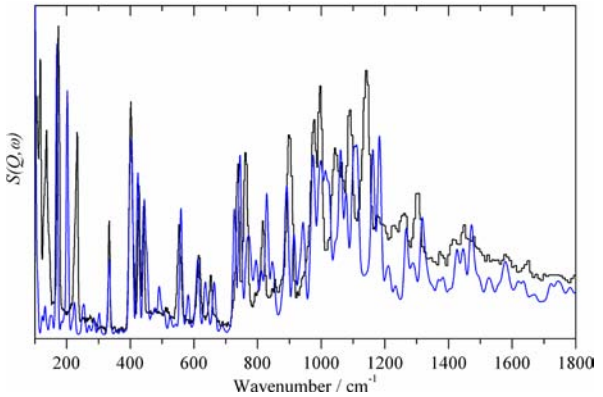

Figure 3. Observed INS spectrum of transoid 2,2′-bipyridine (black trace) and the calculated (blue trace) INS spectrum of the hypothetical cisoid 2,2′-bipyridine.

to the ring−ring torsion (since the space group is $P1$) and consequently this mode falls in energy to 54 cm^{-1}. In principle, this would be expected to be imaginary since it is the coordinate that converts the cisoid to the transoid structure. Supporting Information, Table S4 also lists the transition energies and Raman intensities for the cisoid structure.

C. 2,2′-Bipyridyl Dichloro Platinum(II), Pt(bpy)Cl_2. Pt(bpy)Cl_2 exists as two polymorphs, a red and a yellow form. Structural determinations[35,36] show that the molecular structure is the same in both cases and that the difference in color arises from differences in both the intermolecular packing and the intermolecular Pt···Pt distance that allows a direct Pt to Pt interaction in the red solid.[35] In the present work, we have used the yellow form which has $Z = 8$ with C_1 site symmetry, although the molecular symmetry is very close to C_{2v}. (The red solid has $Z = 2$ with crystallographically imposed C_{2v} molecular symmetry). As with PhSSPh, we optimized the complete unit cell and carried out the vibrational analysis, but to make the Raman calculation tractable we reduced the crystal symmetry to $P1$ and removed seven of the molecules. This was then optimized again and the Raman intensities calculated. As may be seen from Supporting Information, Table S5, the calculated

dx.doi.org/10.1021/ic3011184 | Inorg. Chem. 2012, 51, 9748−9756

structure for $Z = 8$ is in good agreement with the experimental determinations, and elimination of seven molecules does not change the structure of the isolated molecule to any significant degree. The observed INS spectrum of $Pt(bpy)Cl_2$ and the calculated INS spectra for the yellow form with $Z = 8$ and $Z = 1$ are shown in Figure 4. It can be seen that there are only minor

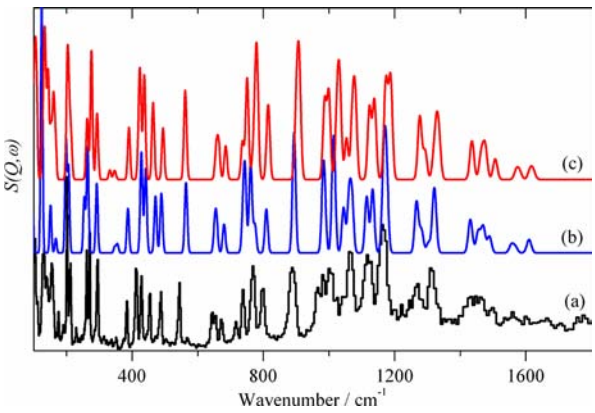

Figure 4. Observed (a) and calculated (b) $Z = 1$, (c) $Z = 8$ INS spectra of 2,2′-bipyridyl dichloro platinum(II), $Pt(bpy)Cl_2$.

differences between the spectra of the $Z = 8$ and $Z = 1$ cases, indicating that the isolated molecule approximation is valid for these weakly interacting systems. The observed and calculated (for $Z = 1$) Raman spectra are shown in Figure 5. In this case

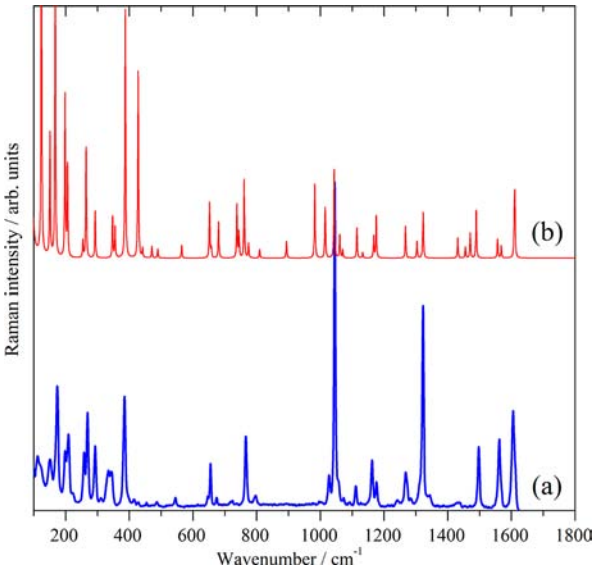

Figure 5. Observed (a) and calculated (b) (for $Z = 1$) Raman spectra of 2,2′-bipyridyl dichloro platinum(II), $Pt(bpy)Cl_2$.

the calculated intensities only poorly reproduce the observed ones. This is probably the result of pre-resonance enhancement of the experimental intensities that are not included in the calculated intensities.

The addition of the $[PtCl_2]$ unit to 2,2′-bipyridine adds an additional nine modes per molecule. These can be categorized as translations of the platinum atom along x, y, and z, which in the molecular context are the symmetric Pt−N stretch (x translation), the asymmetric Pt−N stretch (y translation), and the displacement of the platinum atom perpendicular to the molecular plane (z translation), similar to the umbrella motion of ammonia. The Cl-atoms contribute six modes, that are completely analogous to the modes of a methylene CH_2 group. Thus there are symmetric and asymmetric stretch modes, a scissors mode, and rock, wag, and twist modes, and these are all apparent from the visualizations. Supporting Information, Table S6 lists the observed and calculated transition energies and assignments.

D. 2,2′-Bipyridyl (bis)thiolate platinum(II), Pt(bpy)-$(SPh)_2$ and Pt(d_8-bpy)$(SPh)_2$. The analysis of the spectra of these compounds is severely complicated by the fact that the crystal structure is not known, and all our attempts to obtain suitable crystals were unsuccessful. The related complex $Pt(bpy)(S-C_6F_4\text{-}p\text{-}CN)_2$, (where $S-C_6F_4$-p-CN is 4-cyano-2,3,5,6-tetrafluorothiolate), has been structurally characterized,[37a] and this was used as the starting structure with the fluorines and cyanides replaced by hydrogen. The geometry optimization was very slow because the structure of the complex with the fluorinated thiophenolate ligand is stabilized by a $\pi-\pi$ interaction between the thiolate rings. This interaction is not present in the hydrogen analogue, and the rings could be seen to be slowly drifting apart. To circumvent this problem, the structure was first optimized using Gaussian03, and the resulting structure used as the starting structure for the CASTEP calculation. The resultant energy minimized structure is shown in Figure 6. Table 1 compares selected bond distances and angles with related compounds,[37b,38−40] and it can be seen that the calculated structural parameters are in good agreement with relevant experimental and theoretical values. In particular, the overall geometry of the phenyl rings above and below the plane of the Pt-bpy is very similar to that found experimentally for the closely related complex Pt(d*t*bbpy)(S-4-py)$_2$, (di-*tert*-butylbipyridine)bis-(pyridine-4-thiolato)platinum(II).[37b]

The vibrational analysis shows the first six modes to be external modes, two of which are imaginary modes at −19 and −10 cm^{-1}. Since these are librations of a hypothetical structure, this is not surprising. The internal modes are all real suggesting that the molecular geometry is a reasonable approximation to the (unknown) real structure. Supporting Information, Table S7 lists the observed and calculated transition energies and assignments for both $Pt(bpy)(SPh)_2$ and Pt(d_8-bpy)$(SPh)_2$ and the spectra are shown in Figures 7 and 8. It can be seen that the observed and calculated INS spectra are in excellent agreement, demonstrating that the assignments in Supporting Information, Table S7 are reliable. The calculated Raman spectrum of the fully hydrogenous complex is in poor agreement with the experimental data, again probably because of pre-resonance effects that are not included in the model.

IV. DISCUSSION

As discussed in the Introduction, the assignment of the low frequency modes where the key metal−ligand framework modes lie is severely complicated by experimental difficulties in their observation as well as by intermode coupling. We give a brief survey of the related literature data available for some Pt(II) diimine and thiolate compounds in the region below 500 cm^{-1}, before proceeding to our results.

In Pt(II) complexes, the ν(Pt−N) vibration has been variously assigned to bands at 260−290, 370−380 cm^{-1} and −417−478 cm^{-1} in the vibrational spectra. Vibrational satellites at 245−251 cm^{-1} in the luminescence spectra of $Pt(qol)_2$ (qol- = 8-quinolinolato-*O*,*N*)) in *n*-alkane Spol'skii matrices were assigned to the Pt−N bond,[39] since similar values (266−257

dx.doi.org/10.1021/ic3011184 | Inorg. Chem. 2012, 51, 9748−9756

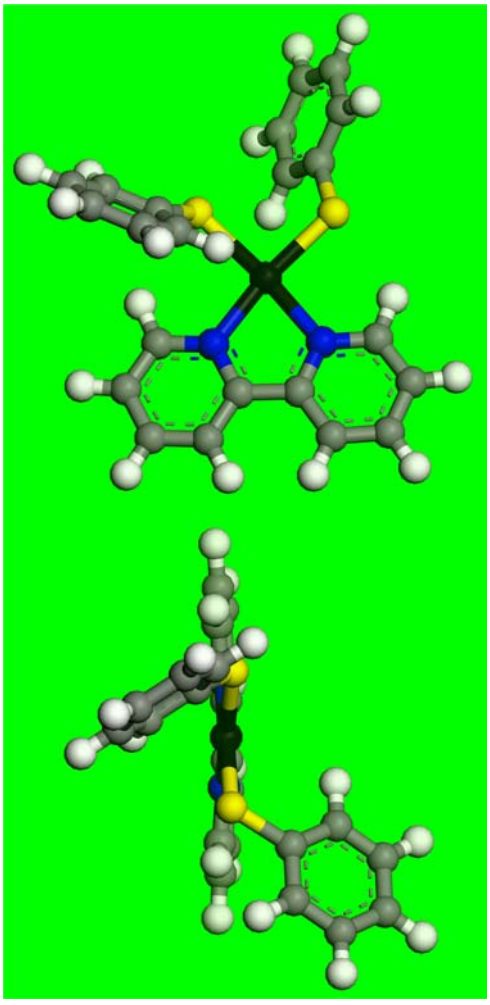

Figure 6. Two views of the CASTEP geometry optimized structure of 2,2′-bipyridyl (bis)thiolate platinum(II), Pt(bpy)(SPh)$_2$.

cm^{-1}) were reported for Cu−N vibrations in the infrared spectra of Cu compounds.[40] For [Pt(bpy-h$_8$)$_2$]$^{2+}$ and [Pt(h$_8$-bpy)(d$_8$-bpy)]$^{2+}$, on the basis of comparison of resonance Raman data and highly resolved emission spectra obtained at T = 1.3−5 K, the bands observed at 382 cm^{-1} and 226 cm^{-1} were assigned to a bpy mode, and the bands at 417, 437, and 471 cm^{-1} were assigned to Pt−N stretches since these modes did not vary greatly with deuteration of bpy.[41]

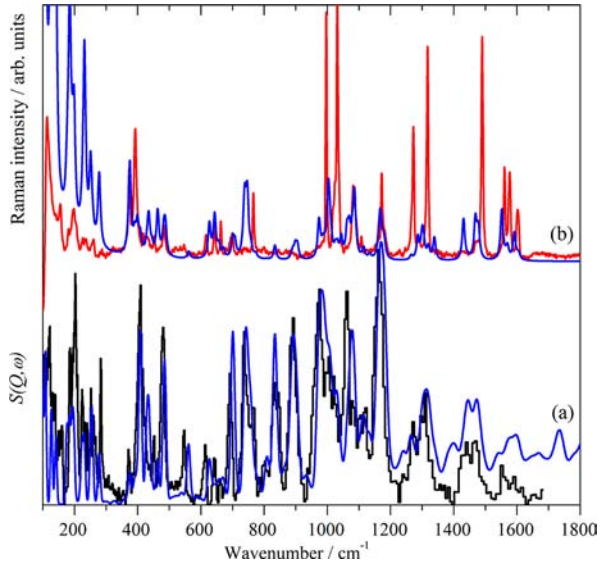

Figure 7. Observed and calculated (a) INS and (b) Raman spectra of 2,2′-bipyridyl (bis)thiolate platinum(II), Pt(bpy)(SPh)$_2$.

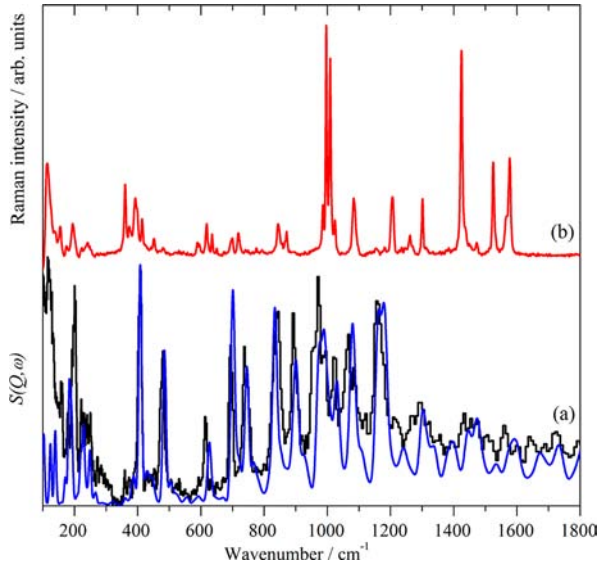

Figure 8. d_8-2,2′-bipyridyl dithiolate platinum(II), Pt(d_8-bpy)(SPh)$_2$: (a) The observed (black trace) and calculated (blue trace) INS spectra and (b) observed Raman spectrum.

Table 1. Comparison of Selected CASTEP Calculated Bond Distances and Angles of 2,2′-Bipyridyl Dithiolate Platinum(II), Pt(bpy)(SPh)$_2$, with Values of Related Compounds

	Pt(bpy)(SPh)$_2$	Pt(bpy)(S−C$_6$F$_4$-p-CN)$_2$	Pt(bpy)Cl$_2$		PtS4[a]	Pt(dtbbpy)(S-4-py)$_2$[b]
	calc[c]	expt.[d]	expt[e]	calc[c]	expt	expt
Pt−N/Å	2.064, 2.076	2.049, 2.054	2.038	2.034		2.057, 2.059
Pt−S/Å	2.290, 2.265	2.2823, 2.2963			2.323, 2.310	2.291, 2.293
S−Aryl/Å	1.747, 1.746	1.747, 1.765			1.761, 1.768	1.742, 1.751
∠N−Pt−N/deg	78.87	79.77	80.9	79.7		79.5
∠S−Pt−S/deg	92.10	92.10			89.95	88.88
∠N−Pt−Scis/deg	96.00, 93.50	92.58, 95.15				174.4, 175.0
∠N−Pt−Strans/deg	174.36, 171.43	170.82, 173.56				96.7, 94.9
∠N−C−C′−N′/deg	0.88	0.43	0.0	2.2		

[a]PtS4 = bis(pentafluorophenylthiolato)-(2,3-bis(methylthio)butane-S,S′)-platinum(II) Pt(CH$_3$SCH(CH$_3$)CH(CH$_3$)SCH$_3$)(S−C$_6$F$_5$)$_2$, ref 38. [b]Pt(dtbbpy)(S-4-py)$_2$ = (di-*tert*-butylbipyridine)bis(pyridine-4-thiolato)platinum(II), ref 37b. [c]This work. [d]Ref 37a. [e]Ref 36.

dx.doi.org/10.1021/ic3011184 | Inorg. Chem. 2012, 51, 9748−9756

For the series of compounds[42] $Pt(thpy)_2$, $Pt(phpz)(thpy)$, and $Pt(SEt_2)I(thpy)$ (thpy = 2′-thienyl-(2-pyridine), phpz = N-phenyl-pyrazole) vibrational satellites were observed at 400, 390, and 390 cm^{-1}, respectively, and hence can be assigned to Pt−N vibrations. For [*cis*-$Pt(glycine)_2$] a strong vibration at 389 cm^{-1} was assigned[7a] to ν(Pt−N).

For the related compounds[43] Ni(baba)(mnt) and Pd(baba)-(mnt), (baba = bisacetylbisaniline, mnt = 1,2-maleonitriledithiolate), the Raman bands at 273 and 258 cm^{-1}, respectively, were attributed to the M−N bond, and hence the Pt−N vibration can be expected at slightly lower wavenumbers, following the tendency observed[44] for $[M(mnt)_2]^{2-}$ with M = Ni^{II}, Pd^{II}, Pt^{II}.

This summary demonstrates that there is a lack of consistency in the assignments of the low frequency framework modes for this group of compounds. The purpose of this study was to assign the vibrational modes of the molecule $Pt(bpy)(PhS)_2$ with particular emphasis on locating the Pt−X (X = N, S) modes, since these are most likely to be involved in dissipating the energy absorbed on photoexcitation.

We begin with the simpler (by virtue of the symmetry) $Pt(bpy)Cl_2$ system and then apply the same methods to the dithiolate complex. To generate the INS spectrum, the ACLIMAX program[22] calculates the amplitude of vibration of each atom from its displacement in each mode; the displacement is weighted by the total scattering cross section. If the cross sections of all the atoms are set to zero, except for the atom(s) of interest, then the result shows which atoms have significant motion in each mode. This process was done separately for the platinum, nitrogen, and chlorine atoms and the results are shown in Figure 9. From the results of such

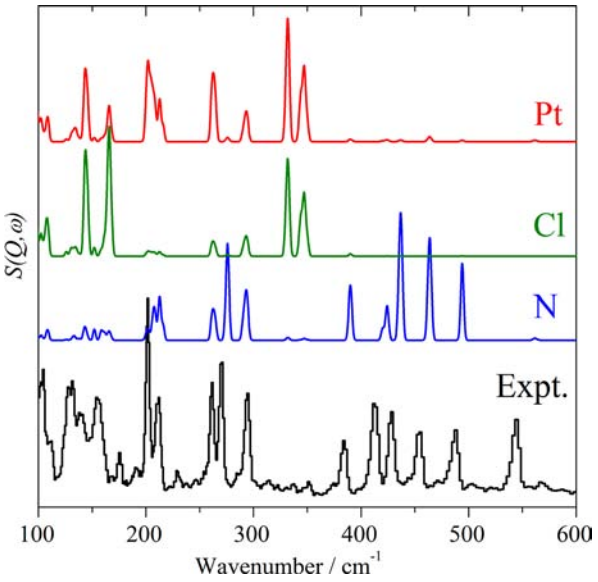

Figure 9. Observed INS spectrum of $Pt(Bpy)Cl_2$ and those calculated considering the N, Cl, and Pt atoms only, which highlight the modes associated with the particular atom.

analyses it is immediately apparent that the Pt−Cl stretch and bend modes are located at 347/331 and 166/144 cm^{-1} respectively. Similarly, the Pt−N stretch modes are at 294 and 261 cm^{-1} and the bending modes are at 214 and 202 cm^{-1}. Since the modes involving nitrogen at >400 cm^{-1} do not cause any significant platinum motion, they must relate to C−N deformations, in agreement with the assignments in Supporting Information, Table S7. We note that this result strongly suggests that the bands at 417, 437, and 471 cm^{-1} in $[Pt(h_8\text{-bpy})_2]^{2+}$ are probably internal bipyridyl modes, rather than Pt−N stretch modes as was suggested previously.[41] Inspection of the spectra in ref 39 shows bands at 227, 245, and 267 cm^{-1} that show only small shifts on deuteration, and these are assigned as the Pt−N stretch modes, consistent with the other complexes listed in Table 2.

The Pt−Cl and Pt−N modes have been previously assigned by comparison of the infrared spectra of a series of $M(bpyX_2)$ complexes (M = Pd, Pt; X = Cl, Br, I) and the corresponding d_8-bpy complexes.[49,50] Our assignments are in complete agreement with the earlier work, see Table 2. It is of relevance to see if the spectral changes on metal and/or halogen substitution are purely mechanical, that is, the result of the change in mass or whether there is an electronic component as well. If the former proposition is correct, then the spectra calculated for the "isotopes" should match those experimentally observed. Table 2 compares the experimental and calculated transition energies. It can be seen that the M−N stretch is largely independent of the halogen and that the M−X transition energies are largely determined by the mass, suggesting that the bonding is very similar in all the cases.

The same procedure was applied to the bis-thiolate complexes, and the results are shown in Figures 10 and 11. It can be seen that the results are much less clear. Many of the modes involve motion of all the atoms, and this is particularly so for the d_8-bpy complex, Figure 11. We believe that there are two main reasons for this phenomenon. First, the molecular symmetry is now C_1 rather than (approximately) C_{2v} for the dihalo complexes; thus, all the modes are allowed to couple by symmetry and, second, the mass of the ligands has greatly increased: 70.9 for the dichloro versus 218.4 for the bis-thiolate. For the latter, the mass is now comparable to that of the platinum atom (195.1); thus the bipyridyl is now mechanically coupled to the thiolates whereas this does not happen for the dichloro complex, in essence the heavy platinum atom isolates the two parts of the complex.

Nonetheless, using mode visualization in particular, and the summary of the literature data given below, some useful conclusions have been drawn on the origin of the low frequency vibrations in the thiolate complexes.

A similar diversity of assignments can be found in the literature with respect to ν(Pt−S) as we discussed above for ν(Pt−N). The Pt−S vibration was reported[7a] to appear at 405 and <310 cm^{-1} for $Pt(S_2C_2Me_2)_2$, 403 and 373 cm^{-1} for $Pt(S_2C_2Ph_2)_2$; 375 and 288 cm^{-1} for $Pt(S_2CNH_2)_2$; 362 and 330 cm^{-1} for $Pt(Me\text{-xanthane})_2$ and 298−350 cm^{-1} for [*cis*-$PtCl_4(SMe_2)_2$].[45]

In the mixed valence Pt^{II}/Pt^{IV} complexes $[Pt(en)(SCN)_2]$-$[Pt(en)(SCN)_2X_2]$, (en = 1,2-ethanediamine and X = I, Br) bands observed at 272.4 and 298.3 cm^{-1} in the resonance Raman spectra were assigned[46] to ν(Pt−S) (and also tentatively 206.6 cm^{-1}), while the bands at 355 and 385 cm^{-1} were assigned to $2\nu_1$(Br−Pt−Br) and to {ν(Br−Pt−Br) + δ(N−Pt−N)}, respectively. In the infrared spectra of these compounds all bands observed in the region 297−339 cm^{-1} were assigned to ν(Pt−S) modes.

In the case of a bis(dithiolate) complex $[Pt(mnt)_2]^{2-}$ the bands at 377.6 and 311.1 cm^{-1} were assigned[44] to Pt−S stretches. The assignment of the 375−380 cm^{-1} polarized vibrational band to a Pt−S stretch was confirmed by analyzing[47] the vibrational satellites in the emission and polarized

dx.doi.org/10.1021/ic3011184 | Inorg. Chem. 2012, 51, 9748−9756

Table 2. Observed and Calculated Transition Energies (cm^{-1}) of Modes with Metal Displacement in the Complexes $M(bpy)X_2$ (M = Pd, Pt, X = Cl, Br, I), $Pt(bpy)(SPh)_2$ and Related Compounds[a]

		M−X stretch		M−X bend		M−N stretch		ref.
complex	X	obs[b]	calc	obs	calc	obs	calc	
$Pd(bpy)I_2$	I	180/161	199/182	102	93	280/208	342/321	49
$Pd(bpy)Br_2$	Br	225/190	223/198	151	121/114	302/290	347/328	49
$Pd(bpy)Cl_2$	Cl	357/344	381/364	172	169/147	279/247	299/276	49
$Pt(bpy)I_2$	I	171/156	193/181	138/101	89	286/195	304/277	49
$Pt(bpy)Br_2$	Br	244/231	239/221	133/113	116/113	331/244	307/282	49
$Pt(bpy)Cl_2$	Cl	350/336	347/331	175/154	165/143	295/260	292/262	49
$Pt(bpy)Cl_2$	Cl	343/333	347/331	175/149	165/143	294/261	292/262	this work
$Pt(bpy)(SPh)_2$	S	393/393[c]	399/390	122	141/128	283/253	278/251	this work
$Pt(d_8\text{-bpy})(SPh)_2$	S	393/393[c]	389/383		140/125	251/241	267/249	this work
$Pt(bpy)(d_8\text{-bpy})$						227/245/267[d]		41
$Pt[(mnt)_2]^{2-}$	S	311/377						44
Pd(baba)(mnt)	S	360				258		43
Ni(baba)(mnt)	S	330				273		43

[a]The calculated transition energies are for $M(bpy)X_2$ with appropriate mass substitutions. [b]Observed transition energies from the literature are from infrared spectra, those from this work are from the INS spectra. [c]From the Raman spectrum. [d]The Pt−N stretch modes are given as 417, 437, and 471 cm^{-1} in ref 41. See text for explanation.

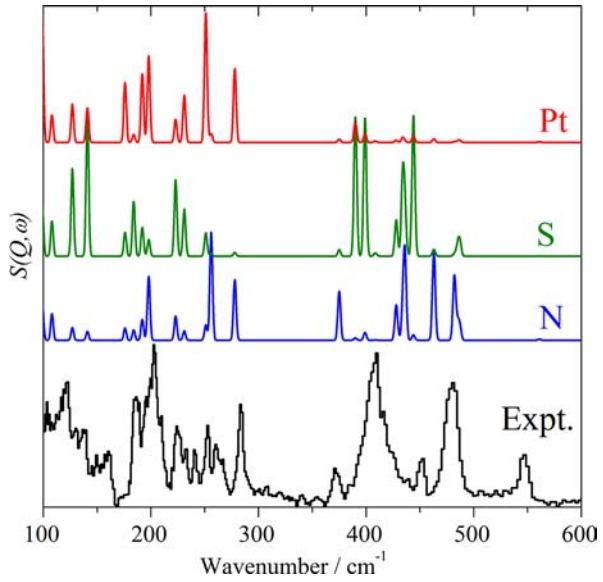

Figure 10. Observed INS spectrum of $Pt(bpy)(SPh)_2$ and those calculated considering the N, S, and Pt atoms only.

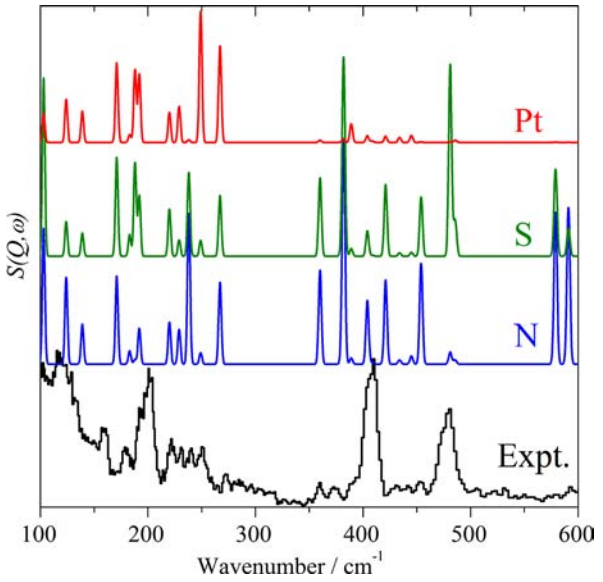

Figure 11. Observed INS spectrum of $Pt(d_8\text{-bpy})(SPh)_2$ and those calculated considering the N, S, and Pt atoms only.

absorption (T = 2 K) spectra of single crystals of $[Bu_4N]_2[Pt(mntS_2)_2]$.

Highly resolved low temperature emission spectra obtained for $Pt(qtl)_2$ (qtl = 8-quinolinethiolato-) in Spols'kii matrices at 1.2 K possess two progression forming bands at 239−242 cm^{-1} and at 361−372 cm^{-1}, which the authors assigned[48] to Pt−N and Pt−S vibrations, respectively. No definite assignment is given for the Pt−S vibration on the basis of vibrational satellites observed in the highly resolved low temperature emission spectra[41] of $Pt(SEt_2)I(thpy)$, although vibrations at 70−90 cm^{-1} were reported as "complex vibrations".

For Ni(baba)(mnt) and Pd(baba)(mnt), wavenumbers at 330 and 360 cm^{-1} were attributed[43] to the M−S bond, and hence Pt−S vibrations can be expected at a slightly higher wavenumbers, following the tendency observed[44] for $[M(mnt)_2]^{2-}$ with $M = Ni^{II}$, Pd^{II}, Pt^{II}.

The INS spectra of $Pt(bpy)(SPh)_2$ and $Pt(d_8\text{-bpy})(SPh)_2$ shown in Figure 10 and 11 along with the spectra emphasizing only Pt, S, or N containing modes, allows for some mode-specific assignment. First, one notes that the most strong and broad bands in the INS spectra do not appear in the Pt, N, or S-only spectra, as could be anticipated, as modes with large amplitude hydrogen motions largely involve the atoms on the periphery of the complex, rather than the $[S_2-Pt-N_2]$ core. Specifically, broad bands appear in the INS spectrum of $Pt(bpy)(SPh)_2$ at 121, 202, 160, 283, 409, and 547 cm^{-1}. The INS spectrum of $Pt(bpy)Cl_2$ (Figure 9) also demonstrates INS bands at 120, 410, and 547 cm^{-1} which do not appear at all in the spectra calculated with only Pt, N, or Cl contribution. Accordingly, those bands are assigned to the bpy-based vibrations. The bands at 547, 283, and 121 cm^{-1} are not present in the experimental INS spectrum of $Pt(d_8\text{-bpy})(SPh)_2$, further supporting their assignment to the bpy-based vibrations. Notably, the bands at 409 cm^{-1} and ~200 cm^{-1} are considerably broader and more intense in the spectrum of $Pt(bpy)(SPh)_2$ as compared to $Pt(bpy)Cl_2$, which indicates a

dx.doi.org/10.1021/ic3011184 | Inorg. Chem. 2012, 51, 9748−9756

considerable contribution of the Ph-ring based vibrations of the −SPh ligand in those bands but which do not involve any appreciable contribution from the S-atoms.

Given the particular emphasis of this study on the framework modes, that is, those involving N, S, and Pt, we will now focus on the assignment of the modes pronounced in the atom-specific N, S, and Pt spectra, which may be weak in the experimental INS spectrum because of the small amplitude of motion of the protons.

The mode visualizations show that all the modes at >400 cm^{-1} are internal modes of the phenyl groups or the bipyridyl ligand. Motion of the Pt, N, or S can result from these, a case in point is the mode at 488 cm^{-1} which is a classic deformation mode of the phenyl ring (20b): since the carbon atom to which the sulfur is bonded is displaced out of the plane of the ring, the sulfur atom must also move in the mode. This effect arises because a requirement of a normal mode is that the center of mass is invariant during the motion.

For modes at <400 cm^{-1} in $Pt(bpy)(SPh)_2$, the vibrational bands which are (almost) exclusive to the motions of the S-atom, that is, do not appear in the spectrum calculated using N or Pt contribution only, and are very weak in the experimental INS spectrum, are at 390 and 399 cm^{-1} and are assigned as ν(Pt−S). In the Raman spectrum a medium band at 393 cm^{-1} is observed that does not shift on deuteration of the bipyridyl ligand, the width of this band is double that of the surrounding bands suggesting the presence of two modes. The calculations suggest that the two Pt−S stretch modes occur at similar energy, so it is likely that they are not resolved in the experimental Raman spectrum. Similarly, the modes at 278 and 251 cm^{-1} can be assigned as a Pt−N stretch. Surprisingly, the antisymmetric Pt−N stretch at 251 cm^{-1} only appears very weakly; the adjacent strong mode at 258 cm^{-1} is an out-of-plane motion of the bipyridyl that results in considerable displacement of the nitrogen atoms. The presence of these bands in the INS spectrum of $Pt(bpy)Cl_2$ calculated in the "N-only" mode support this assignment. At lower energy, most of the modes exhibit a moderate contribution from both N and S, with variable contribution from the Pt atom and can be assigned as strongly coupled deformations of the $[S_2-Pt-N_2]$ framework.

For the deuterated analogue, $Pt(d_8\text{-}bpy)(SPh)_2$, the calculations predict that ν(Pt−S) is at 389/393 cm^{-1}, very close to the 393 cm^{-1} observed in the Raman spectrum. Interestingly, no modes specific to the Pt−N contribution have been detected—all modes involving N contribution also involve that from S. Overall, as with the fully protonated complex, all the modes detected in the range 390−103 cm^{-1} can be assigned as coupled $[S_2-Pt-N_2]$ modes with variable contribution from S, N, and Pt. This observation implies a somewhat larger degree of coupling in case of the $Pt(d_8\text{-}bpy)(SPh)_2$ if compared to $Pt(bpy)(SPh)_2$. Overall, despite severe coupling in the low frequency region, the combination of INS and Raman spectra supported by periodic-DFT calculations have allowed us to assign several Pt−S and Pt−N specific modes in the case of the Pt(II) diimine thiolate complex, $Pt(bpy)(SPh)_2$.

V. CONCLUSIONS

A combination of inelastic neutron scattering and Raman methods (Figures 10 and 11) with the aid of the mode visualizations allowed for an identification of the modes that contain significant contributions from Pt−S and Pt−N stretch modes (Table 2). For Pt−S the stretches are located near 400 cm^{-1} and for Pt−N in a wide range of complexes these occur in the 250−300 cm^{-1} range. The results also demonstrate that it is extremely difficult to assign transition energies to "pure", localized modes in the low frequency region, as a consequence of the anticipated severe mixing that occurs among the skeletal modes. The modes involving sulfur motion are relatively weak in the Raman spectrum, but observable. For the higher energy modes that relate to the internal motions of the phenyl and bipyridyl groups these conform to the expected patterns.[25−27,31,32] The use of INS has proved invaluable in identifying and assigning the modes in the lowest frequency region, and overall the results will be of assistance in analyzing the structure of the electronic excited state in chromophores containing a Pt(diimine) core essential to understanding of their photoreactivity.

■ ASSOCIATED CONTENT

Supporting Information

Further details are given in Tables S1−S7. This material is available free of charge via the Internet at http://pubs.acs.org.

■ AUTHOR INFORMATION

Corresponding Author

*E-mail: stewart.parker@stfc.ac.uk (S.F.P.), julia.weinstein@sheffield.ac.uk (J.A.W.).

Notes

The authors declare no competing financial interest.

■ ACKNOWLEDGMENTS

We thank the STFC Rutherford Appleton Laboratory for access to neutron beam facilities, EPSRC (Advanced Research Fellowship to J.A.W.), RFBR and the University of Sheffield for support. Computing resources (time on the SCARF computer used to perform the CASTEP calculations) was provided by STFC's e-Science facility. We are indebted to Prof. H. Vos (Dublin City University, Ireland), and Prof. O. Poizat (Université de Lille I, France), who kindly provided some of the per-deuterated ligands.

■ REFERENCES

(1) (a) Hammarstrom, L.; Winkler, J. R.; Gray, H. B.; Styring, S. *Science* **2011**, *333*, 288. (b) Alstrum-Acevedo, J. H.; Brennaman, M. K.; Meyer, T. J. *Inorg. Chem.* **2005**, *44*, 6802−6827. Eisenberg, R. *Science* **2009**, *324*, 44.

(2) See for example Solar Energy Forum, *Inorg. Chem.*, **2005**, 44, all articles, Falkenstrom, M.; Johansson, O.; Hammarstrom, L. *Inorg. Chim. Acta* **2007**, *360*, 741−750.

(3) (a) Sazanovich, I. V.; Alamiry, M. A. H.; Best, J.; Bennett, R. D.; Bouganov, O. V.; Davies, E. S.; Grivin, V. P.; Meijer, A. J. H. M.; Plyusnin, V. F.; Ronayne, K. L.; Tikhomirov, S. A.; Towrie, M.; Weinstein, J. A. *Inorg. Chem.* **2008**, 10432−10445. (b) Muro, M. L.; Rachford, A. A.; Wang, X.; Castellano, F. N. *Top. Organomet. Chem.* **2010**, *29*, 159−191. (c) Guo, F.; Ogawa, K.; Kim, Y.-G.; Danilov, E. O.; Castellano, F. N.; Reynolds, J. R.; Schanze, K. S. *Phys. Chem. Chem. Phys.* **2007**, *9*, 2724−2734. (d) Chan, C. K. M.; Tao, C.-H.; Li, K.-F.; Man-Chung Wong, K.; Zhu, N.; Cheah, K.-W.; Yam, V. W.-W. *J. Organomet. Chem.* **2011**, *696*, 1163−1173. (e) Guo, F.; Kim, Y.-G.; Reynolds, J. R.; Schanze, K. S. *Chem. Commun.* **2006**, 1887−1889. (f) Wadas, T. J.; Chakraborty, S.; Lachicotte, R. J.; Wang, Q.-M.; Eisenberg, R. *Inorg. Chem.* **2005**, *44*, 2628−2638. (g) McGarrah, J. E.; Eisenberg, R. *Inorg. Chem.* **2003**, *42*, 4355−4365. (h) McGarrah, J. E.; Kim, Y. J.; Hissler, M.; Eisenberg, R. *Inorg. Chem.* **2001**, *40*, 4510−4511. (i) Whittle, C. E.; Weinstein, J. A.; George, M. W.; Schanze, K. S. *Inorg. Chem.* **2001**, *40*, 4053−4062. (j) Hissler, M.; Connick, W. B.;

Geiger, D. K.; McGarrah, J. E.; Lipa, D.; Lachicotte, R. J.; Eisenberg, R. *Inorg. Chem.* **2000**, *39*, 447−457. (k) Hissler, M.; McGarrah, J. E.; Connick, W. B.; Geiger, D. K.; Cummings, S. D.; Eisenberg, R. *Coord. Chem. Rev.* **2000**, *208*, 115−137. (l) Connick, W. B.; Miskowski, V. M.; Houlding, V. H.; Gray, H. B. *Inorg. Chem.* **2000**, *39*, 2585−2592. (m) Archer, S.; Weinstein, J. A. *Coord. Chem. Rev.* **2012**, DOI: 10.1016/j.ccr.2012.07.010. (n) Islam, A.; Sugihara, H.; Hara, K.; Singh, L. P.; Katoh, R.; Takahashi, Y.; Murata, S.; Arakawa, H. *New J. Chem.* **2000**, *24*, 343−345. (o) Geary, E. A .M.; Yellowlees, L. J.; Jack, L. A.; Oswald, I. D. H.; Parsons, S.; Hirata, N.; Durrant, J. R.; Robertson, N. *Inorg. Chem.* **2005**, *44*, 242−250. (p) Zhang, J.; Du, P.; Schneider, J.; Jarosz, P.; Eisenberg, R. *J. Am. Chem. Soc.* **2007**, *129*, 7726.

(4) (a) Best, J.; Sazanovich, I. V.; Adams, H.; Bennett, R. D.; Davies, E. S.; Meijer, A. J. H. V.M; Towrie, M.; Tikhomirov, S. A.; Bouganov, O. V.; Ward, M. D.; Weinstein, J. A. *Inorg. Chem.* **2010**, *49*, 10041−10056. (b) Glik, E. A.; Kinayyigit, S.; Ronayne, K. L.; Towrie, M.; Sazanovich, I. V.; Weinstein, J. A.; Castellano, F. N. *Inorg. Chem.* **2008**, *47*, 6974−6983. (c) Adams, C. J.; Harison, Z.; Fey, N.; Sazanovich, I. V.; Towrie, M.; Weinstein, J. A. *Inorg. Chem.* **2008**, *47*, 8242−8257. (d) Shavaleev, N. M.; Adams, H.; Best, J.; Davies, E. S.; Weinstein, J. A. *Inorg. Chem.* **2008**, *47*, 1532−1547.

(5) (a) Schoonover, J. R.; Strouse, G. F. *Chem. Rev.* **1998**, *98*, 1335−1356. (b) Barbara, P. F.; Meyer, T. J.; Ratner, M. A. *J. Phys. Chem.* **1996**, *100*, 13148−13168.

(6) Zink, J. I.; Shin, K.-S. K. Molecular Distortions in Excited Electronic States Determined from Electronic and Resonance Raman Spectroscopy. In *Advances in Photochemistry*; Volman, D. H., Hammond, G. S., Neckers, D. C., Eds.; John Wiley & Sons, Inc.: Hoboken, NJ, 2007; Vol. *16*, doi: 10.1002/9780470133460.ch3

(7) (a) Adams, D. M. *Metal-Ligand and Related Vibrations*; Edward Arnold: London, U.K., 1967; (b) Nakamoto, K. *Infrared and Raman Spectra of Inorganic and Coordination Compounds. Part B: Applications in Coordination, Organometallic and Bioinorganic Chemistry*, 5th ed.; Wiley-Interscience: New York, 1997.

(8) Mitchell, P. C. H.; Parker, S. F.; Ramirez-Cuesta, A. J.; Tomkinson, J. *Vibrational Spectroscopy with Neutrons: With Applications in Chemistry, Biology, Materials Science, and Catalysis*; World Scientific: Singapore, 2005.

(9) Parker, S. F. *Coord. Chem. Rev.* **2010**, *254*, 215−234.

(10) (a) Parker, S. F.; Forsyth, J. B. *J. Chem. Soc. Faraday Trans.* **1998**, *94*, 1111−1114. (b) Parker, S. F.; Herman, H.; Zimmerman, A.; Williams, K. P. J. *Chem. Phys.* **2000**, *261*, 261−266.

(11) de Carvalho, L. A. E. B.; Marques, M. P. M.; Parker, S. F.; Tomkinson, J. *ChemPhysChem* **2011**, *12*, 1334−1341.

(12) (a) Weinstein, J. A.; Zheligovskaya, N. N.; Mel'nikov, M. Ya.; Hartl, F. *J. Chem. Soc., Dalton Trans.* **1998**, 2459−2466. (b) Morgan, G. T.; Burstall, F. H. *J. Chem. Soc.* **1934**, 965.

(13) Colognesi, D.; Celli, M.; Cilloco, F.; Newport, R. J.; Parker, S. F.; Rossi-Albertini, V.; Sacchetti, F.; Tomkinson, J.; Zoppi, M. *Appl. Phys. A: Mater. Sci. Process* **2002**, *74*, S64.

(14) www.isis.stfc.ac.uk.

(15) Adams, M. A.; Parker, S. F.; Fernandez-Alonso, F.; Cutler, D. J.; Hodges, C.; King, A. *Appl. Spectrosc.* **2009**, *63*, 727.

(16) Clark, S. J.; Segall, M. D.; Pickard, C. J.; Hasnip, P. J.; Probert, M. J.; Refson, K.; Payne, M. C. *Z. Kristallogr.* **2005**, *220*, 567.

(17) Refson, K.; Tulip, P. R.; Clark, S. J. *Phys. Rev. B* **2006**, *73*, 155114.

(18) Perdew, J.; Burke, K.; Ernzerhof, M. *Phys. Rev. Lett.* **1996**, *77*, 3865.

(19) Milman, V.; Perlov, A.; Refson, K.; Clark, S. J.; Gavartin, J.; Winkler, B. *J. Phys.: Condens. Matter* **2009**, *21*, 485404.

(20) Refson, K. *Phonons and Related Calculations in CASTEP*, http://www.castep.org/

(21) Frisch, M. J.; Trucks, G. W.; Schlegel, H. B.; Scuseria, G. E.; Robb, M. A.; Cheeseman, J. R.; Montgomery, Jr., J. A.; Vreven, T.; Kudin, K. N.; Burant, J. C.; Millam, J. M.; Iyengar, S. S.; Tomasi, J.; Barone, V.; Mennucci, B.; Cossi, M.; Scalmani, G.; Rega, N.; Petersson, G. A.; Nakatsuji, H.; Hada, M.; Ehara, M.; Toyota, K.; Fukuda, R.; Hasegawa, J.; Ishida, M.; Nakajima, T.; Honda, Y.; Kitao, O.; Nakai, H.; Klene, M.; Li, X.; Knox, J. E.; Hratchian, H. P.; Cross, J. B.; Bakken, V.; Adamo, C.; Jaramillo, J.; Gomperts, R.; Stratmann, R. E.; Yazyev, O.; Austin, A. J.; Cammi, R.; Pomelli, C.; Ochterski, J. W.; Ayala, P. Y.; Morokuma, K.; Voth, G. A.; Salvador, P.; Dannenberg, J. J.; Zakrzewski, V. G.; Dapprich, S.; Daniels, A. D.; Strain, M. C.; Farkas, O.; Malick, D. K.; Rabuck, A. D.; Raghavachari, K.; Foresman, J. B.; Ortiz, J. V.; Cui, Q.; Baboul, A. G.; Clifford, S.; Cioslowski, J.; Stefanov, B. B.; Liu, G.; Liashenko, A.; Piskorz, P.; Komaromi, I.; Martin, R. L.; Fox, D. J.; Keith, T.; Al-Laham, M. A.; Peng, C. Y.; Nanayakkara, A.; Challacombe, M.; Gill, P. M. W.; Johnson, B.; Chen, W.; Wong, M. W.; Gonzalez, C.; Pople, J. A. *Gaussian 03*, Revision B.05; Gaussian, Inc.: Wallingford, CT, 2004.

(22) Ramirez-Cuesta, A. J. *Comput. Phys. Commun.* **2004**, *157*, 226.

(23) Shimizu, T.; Isono, H.; Yasui, M.; Iwasaki, F.; Kamigata, N. *Org. Lett.* **2001**, *3*, 3639.

(24) Räisänen, M. T.; Runeberg, N.; Klinga, M.; Nieger, M.; Bolte, M.; Pyykkö, P.; Leskelä, M.; Repo, T. *Inorg. Chem.* **2007**, *46*, 9954 , and Supporting Information.

(25) Allum, K. G.; Creighton, J. A.; Green, J. H. S.; Minkoff, G. J.; Prince, L. H. S. *Spectrochim. Acta* **1968**, *24A*, 927.

(26) Green, J. H. S. *Spectrochim. Acta* **1968**, *24A*, 1627.

(27) Tolaieb, B.; Aroca, R. *Can. J. Anal. Sci. Spec.* **2002**, *48*, 139.

(28) Almenningen, A.; Bastiansen, O.; Gundersen, S.; Samdal, S. *Acta Chem. Scand.* **1989**, *43*, 932.

(29) Kühn, F. E.; Groarke, M.; Bencze, E.; Herdtweck, E.; Prazeres, A.; Santos, A. M.; Calhorda, M. J.; Romão, C. C.; Gonçalves, I. S.; Lopes, A. D.; Pillinger, M. *Chem.—Eur. J.* **2002**, *8*, 2370.

(30) Kaes, C.; Katz, A.; Hossein, M. W. *Chem. Rev.* **2000**, *100*, 3553.

(31) Neto, N.; Muniz-Miranda, M.; Angeloni, L.; Castellucci, E. *Spectrochim. Acta* **1983**, *39A*, 97.

(32) Ould-Moussa, L.; Castella-Ventura, M.; Kassab, E.; Poizat, O.; Strommen, D. P.; Kincaid, J. R. *J. Raman Spectrosc.* **2000**, *31*, 377.

(33) Muniz-Miranda, M.; Castellucci, E.; Neto, N.; Sbrana, G. *Spectrochim. Acta* **1983**, *39A*, 107.

(34) Muniz-Miranda, M.; Cardini, G.; Castellucci, E. *J. Raman Spectrosc.* **1990**, *21*, 495.

(35) Connick, W. B.; Henling, L. M.; Marsh, R. E.; Gray, H. B. *Inorg. Chem.* **1996**, *35*, 6261.

(36) Canty, A. J.; Skelton, B. W.; Traill, P. R.; White, A. H. *Aust. J. Chem.* **1992**, *45*, 417.

(37) (a) Weinstein, J. A.; Blake, A. J.; Davies, E. S.; Davis, A. L.; George, M. W.; Grills, D. C.; Lileev, I. V.; Maksimov, A. M.; Matousek, P.; Mel'nikov, M. Ya.; Parker, A. W.; Platonov, V. E.; Towrie, M.; Wilson, C.; Zheligovskaya, N. N. *Inorg. Chem.* **2003**, *42*, 7077. (b) Paw, W.; Lachicotte, R. J.; Eisenberg, R. *Inorg. Chem.* **1998**, *37*, 4139−4141.

(38) Martin, E.; Toledo, B.; Torrens, H.; Lahoz, F.; Terreros, P. *Polyhedron* **1998**, *17*, 4091.

(39) Donges, D.; Nagle, J. K.; Yersin, H. *Inorg. Chem.* **1997**, *36*, 3040−3048.

(40) Goldstein, M.; Mooney, E. F.; Anderson, A.; Gebbie, H. A. *Spectrochim. Acta* **1965**, *21*, 105.

(41) Humbs, W.; Yersin, H. *Inorg. Chim. Acta* **1997**, *365*, 139−147.

(42) Stückl, A. C. *Coord. Chem. Rev.* **1997**, *159*, 407.

(43) Wootton, J. L.; Zink, J. I. *J. Phys. Chem.* **1995**, *99*, 7251−7257.

(44) Clark, R. J. H.; Tortule, P. C. *J. Chem. Soc., Dalton Trans.* **1977**, 2142.

(45) Adams, D. M.; Chandler, P. J. *J. Chem. Soc. A* **1967**, 1009.

(46) Clark, R. J. H.; Croud, V. B. *J. Chem. Soc., Dalton Trans.* **1988**, 73.

(47) Guntner, W.; Gliemann, G. *J. Phys. Chem.* **1990**, *94*, 618.

(48) Donges, D.; Nagle, J. K.; Yersin, H. *J. Lumin.* **1997**, *72*−*74*, 658.

(49) Engelter, C.; Thornton, D. A. *Transition Met. Chem.* **1990**, *15*, 212.

(50) Thornton, D. A.; Engelter, C. *J. Coord. Chem.* **1992**, *25*, 299.